RANDOM SEQUENCE FOR OPTIMAL LOW-POWER LASER GENERATED ULTRASOUND

IOP Conf. Series: Journal of Physics: Conf. Series **882** (2017) 012013 doi:10.1088/1742-6596/882/1/012013

RANDOM SEQUENCE FOR OPTIMAL LOW-POWER LASER GENERATED ULTRASOUND

D. Vangi[a], A. Virga[a], M. S. Gulino[a,b]

a. Università degli Studi di Firenze, Department of Industrial Engineering

b. michelangelo.gulino@unifi.it

Abstract. Low-power laser generated ultrasounds are lately gaining importance in the research world, thanks to the possibility of investigating a mechanical component structural integrity through a non-contact and Non-Destructive Testing (NDT) procedure. The ultrasounds are, however, very low in amplitude, making it necessary to use pre-processing and post-processing operations on the signals to detect them. The cross-correlation technique is used in this work, meaning that a random signal must be used as laser input. For this purpose, a highly random and simple-to-create code called T sequence, capable of enhancing the ultrasound detectability, is introduced (not previously available at the state of the art). Several important parameters which characterize the T sequence can influence the process: the number of pulses N_{pulses}, the pulse duration δ and the distance between pulses d_{pulses}. A Finite Element FE model of a 3 mm steel disk has been initially developed to analytically study the longitudinal ultrasound generation mechanism and the obtainable outputs. Later, experimental tests have shown that the T sequence is highly flexible for ultrasound detection purposes, making it optimal to use high N_{pulses} and δ but low d_{pulses}. In the end, apart from describing all phenomena that arise in the low-power laser generation process, the results of this study are also important for setting up an effective NDT procedure using this technology.

1. INTRODUCTION

Ultrasounds (USs) are commonly used in the Non-Destructive-Testing (NDT) field to investigate upon the structural integrity of materials [1,2]. The more utilized instruments for this kind of inspection are narrow band, piezoelectric probes which need the contact with the inspected object to be guaranteed. Non-contact applications use high-power pulsed lasers as a source of elastic waves [3-6], mainly in order to allow an on-line inspection [7]. These waves are generated by the material expansion and contraction due to the laser quick heating and the subsequent sudden cooling. The ultrasonic generated frequencies reach hundreds of MHz, since the laser pulse is typically few nanoseconds long. In order to carry on a definitely NDT procedure while obtaining the highest ultrasonic amplitude possible, the power density is usually kept close to the material's ablative threshold (around $20\ MW/cm^2$ for steel [3]). The ultrasonic amplitudes thus generated, often higher in comparison to the piezoelectric probes ones, make the US detection easy without particular signal manipulations. In some other cases, post-processing techniques can be used, the most recent ones featuring cross-correlation [8] and Laser Nonlinear Wave Modulation Spectroscopy (LNWMS) [9].

Pulsed lasers, such as Nd:YAG, are extremely expensive and particularly bulky; in addition, pulsed lasers spread the energy in a wide range of frequencies, and thus a large energy amount is outside of the receiving probe band too. Recent advances in low-power Continuous Wave (CW) laser diodes technology, which is very important in the medical research field, opened the path to NDT procedures which can guarantee the integrity of the materials, even low melting point ones as composites, making use of a simple, small and low-cost testing layout.

Low-power CW laser diodes have some disadvantages, the main one being a low Signal-to-Noise Ratio (SNR) in the generated US due to the low power used. In order to enhance the SNR, particular modulation sequences are usually employed, which have 2 principal features:

- the sequence consists of a large amount of pulses, since one single pulse cannot generate an ultrasonic oscillation detectable by the instruments (less than 1 pm [10]);
- the sequence is extremely random to accurately characterize the US in Time-Of-Flight (TOF) and Peak-to-Peak (PtP) terms using cross-correlation techniques [11,12].

Low-power laser US are generated feeding (driving) the diode with TTL signals, especially Pseudo-Noise (PN) or pseudo-random sequences [10-15], consisting of several pulses with different lengths. PN codes have a perfectly centred auto-correlation, because of their high randomness characteristic; however, even if this can be an advantage considering only the cross-correlation post-processing purpose, pulses with different durations generate an US with different frequency content [16].

The purpose of this study is to analyse low-power laser generated USs from the thermo-elastic and experimental point of view, considering longitudinal waves propagation inside a 3 mm steel disk. Finite Element (FE) models allow to indagate the features of low-power laser US as can be done in those cases in which high power lasers are used [17-19]. FE analysis does not cover the experimental practice, where a high number of pulses and high randomness in the TTLs driving the laser are necessary [15, 20]: an optimum in SNR can be reached adjusting parameters directly connected to the ultrasonic PtP value and the input sequence's randomness.

PN codes are not flexible because, once their length has been set, there is no way to change the sequence. For this reason, a new highly random sequence has been created, called T-sequence (T stands for "Train of pulses"). It is not present at the state of the art and it gives the researchers the possibility to change as many TTL's parameters as possible.

It will be shown that a proper choice of the influencing parameters can lead to the detection of the US even without using PN codes, which many past studies considered as a basis. The change in the T-sequence's fundamental parameters will be analysed; the best combination of these parameters will be the one which allows to increase SNR the most. Even if the results of a testing campaign (and of FE simulations) on a 3 mm thick steel disk are reported, results relatively close to these can be achieved for a 20 mm thick disk; because of this and other arising phenomena that will be described, it can be assessed that resonances inside the specimen are not always important but only in some particular circumstances.

2. MATERIAL AND EXPERIMENTAL METHOD

2.1. Material

The experimental layout, visible in figure 1, consists of:

- a modulable CW laser diode (TOPTICA iBeam Smart 640 S, 3B class) with a power of 150 mW and wavelength equal to 639 nm;
- a 75 mm focal length spherical lens with reflectivity coefficient R≅0.5%;
- 2 steel disks– with 3 mm and 20 mm thickness- are considered throughout the study (the 20 mm one is shown in the picture);
- a broadband (from 100 kHz to 1 MHz) Brüel & Kjær acoustic probe attached to the steel disk's surface which is opposite to the one irradiated by the laser.

The obtainable focus for the laser was measured by means of a CMOS sensor and resulted in a 30 μm beam waist. The power density is equal to $0.02\ MW/cm^2$ in this configuration, being under the material's ablative threshold [3].

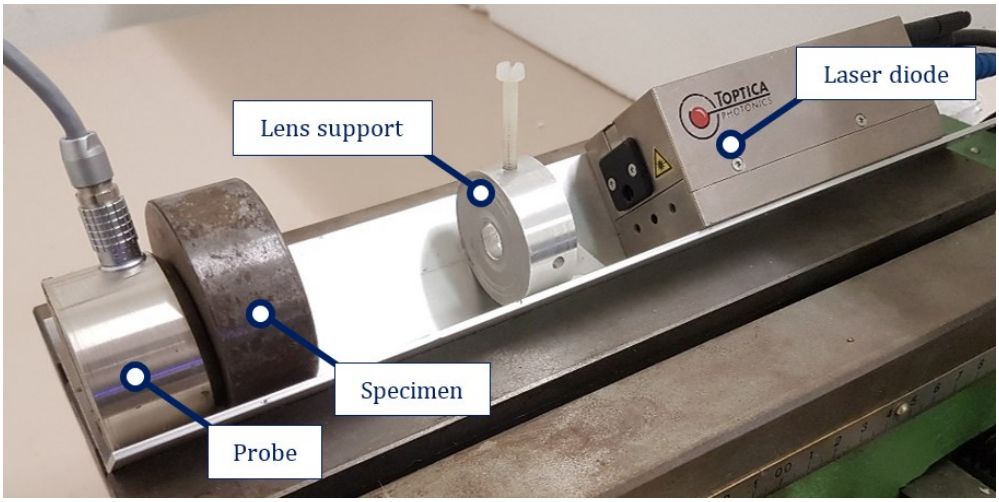

Figure 1. Experimental layout used in the testing procedure.

2.2. T sequence

The US detection in this kind of application mostly depends on signal post-processing techniques: in this context, the cross-correlation algorithm was chosen because of its versatility and use in many other studies on the topic [10-13]. Its application can be effective only if highly random signals are used as laser inputs [15]: the most widely used sequences for this application are PN codes [10-14]. PN codes are extremely random but the thermo-elastic effect is not optimized, because of the difference in each laser pulse length. This is evident considering that they were created for spreading the spectrum in a system [16].

In the ultrasonic field, piezoelectric contact or air-coupled narrow band probes are commonly employed, meaning that a spread spectrum is inefficient for this NDT purpose. PN codes (e.g. Golay codes and M sequences [10,14]) have a precise order in ON/OFF lengths too, so that the only sequences' parameters that can be modified are the length in terms of point and the length in terms of time [15].

To conjugate the necessity of having an output narrow band and a flexible input sequence, a particular sequence was created which is not present in other studies at the state of the art: the T sequence (where T stands for "Train of pulses"). Basically, the T sequence is a signal which possesses equal ON lengths for all pulses, while OFF lengths are created randomly. Every time a T sequence is created through this algorithm, the result can be different. The T sequence in fact represents a category of signals, rather than a single sequence.

The first 50 points of a 6500 points long T sequence are shown in figure 2a. The randomness of the T sequence is visualized through the histogram in figure 2b, where the OFF lengths statistical frequency $p(OFF)$ has a trend comparable to the distribution for the white noise (flat histogram). While PN codes possess an autocorrelation perfectly "centred" (different from 0 only at point 0), the T sequence's auto-correlation (figure 2c) has a minimum adjacent to the maximum. The T sequence, so, is random but also less performing in respect to the PN codes from a randomness point of view. In the next paragraphs, only the cases where this particular T sequence is applied are considered, if not differently specified.

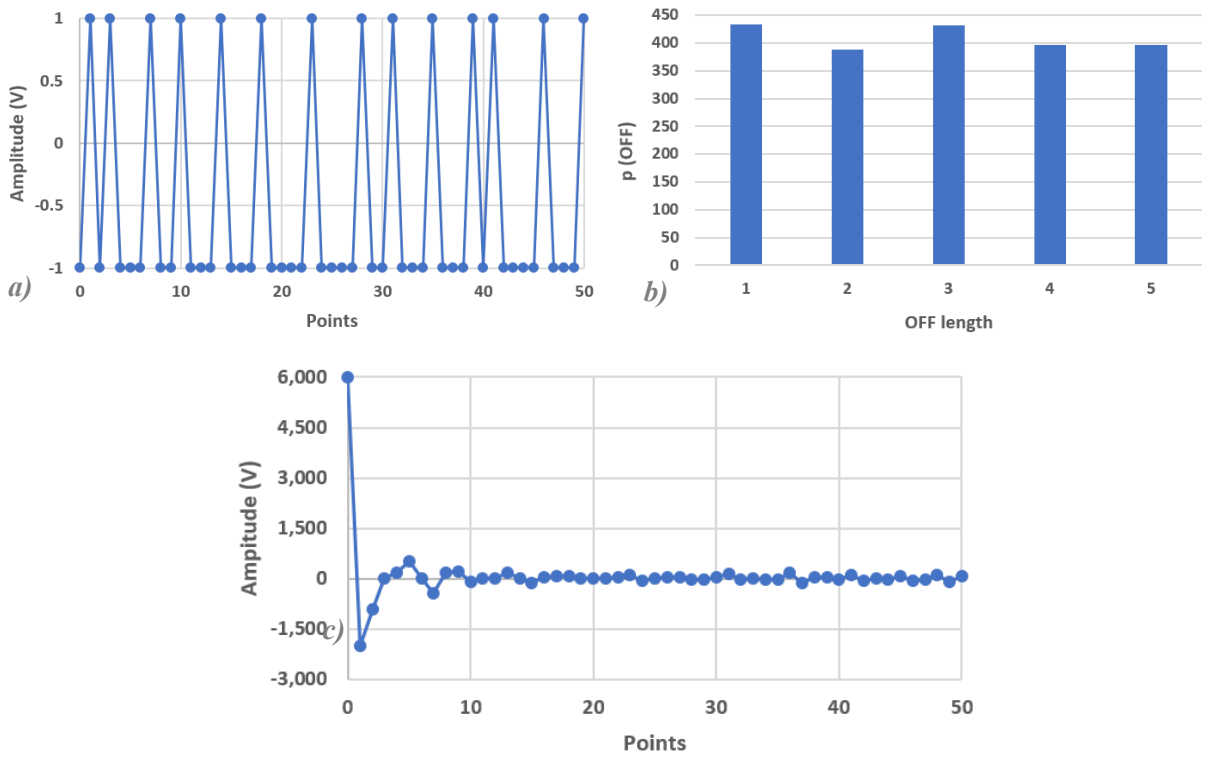

Figure 2. Portion of the T-sequence (a); its randomness is highlighted through the OFF lengths statistical frequency $p(OFF)$ (b) and part of the related auto-correlation (c).

2.3. Method

As a reference, figure 3 shows the steps taken to carry out the testing campaign. First of all, the T-sequence's parameters must be chosen (a); the sequence is generated through a programmable pulse generator (b) and imposed to the laser. The input sequence and the output response to the laser excitation, in which the US is hidden, are displayed on an oscilloscope. The instrument then applies a defined number of ensemble averages on these two interesting signals, in order to partially mitigate the noise influence (c). The probe output is amplified of 60 dB. After these two signals acquisition, the cross-correlation operation (d) is applied between them [8,11,12], and the ultrasonic TOF and PtP can be evaluated from the cross-correlation output (e).

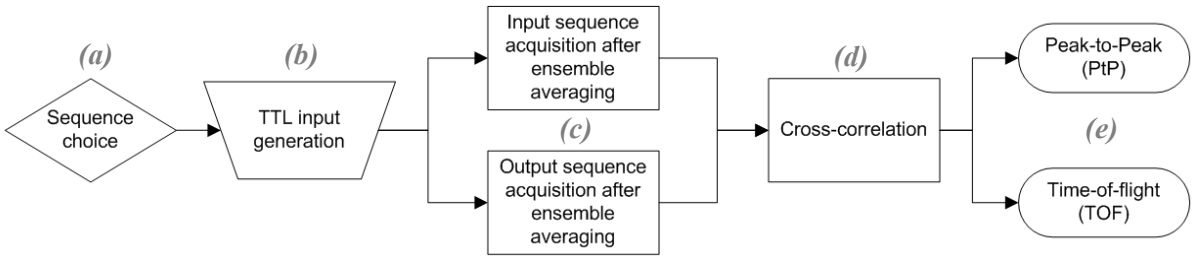

Figure 3. Flow chart regarding the procedure.

Even if SNR can be calculated through a large variety of methods [4,5,8,10,11], it is always represented by the formula:

$$SNR = \frac{Y_{signal}}{Y_{noise}},$$

where Y_{signal} is a generic quantity which considers only the portion of acquired signal interested by the US after the cross-correlation application, while the same applies for the noise with Y_{noise}. The noise is coherent with the generated US, which makes the cross-correlation technique more efficient than other time-frequency methods like Wavelet Transforms [20]. A simple formulation has been considered:

$$Y_{signal} = max(signal) - min(signal) = PtP_{US},$$

$$Y_{noise} = max(noise) - min(noise) = PtP_{noise}.$$

PtP_{US} is calculated on the cross-correlation portion interested by the US and PtP_{noise} on the cross-correlation remaining part.

3. FINITE ELEMENT CHARACTERIZATION

In order to properly study the ultrasonic waves propagation inside a steel disk, a FE analysis regarding the thermo-elastic effect has been carried out through COMSOL© Multiphysics. The laser effect on the material is simulated by a thermal pulse on the disk surface. As the thermal pulse duration is varied, the resulting oscillation's key-features are highlighted.

The pulse duration in the FE analysis will be called δ from now on. Referring to similar works [17-19] which consider high power laser sources, a 2D axisymmetric model has been created (represented in figure 4), allowing to analyse a 3 mm thick revolution solid model without meshing its complete shape. The region close to the axis is the most defined in the r and z directions, with 5 µm wide elements: a particularly high accuracy is needed here, the ipocentre, because of the presence of the laser irradiation with a 15 µm spot radius (the experimentally measured beam-waist). The peripheral one, on the other hand, is coarser and made up of 150 µm wide elements: at the edge, a fixed-end constraint is imposed, as in the experimental layout (disk fixed in respect to a L-shape bar). In the z direction, dimensions vary linearly with the increasing distance. These sizes allowed to minimize the calculation time.

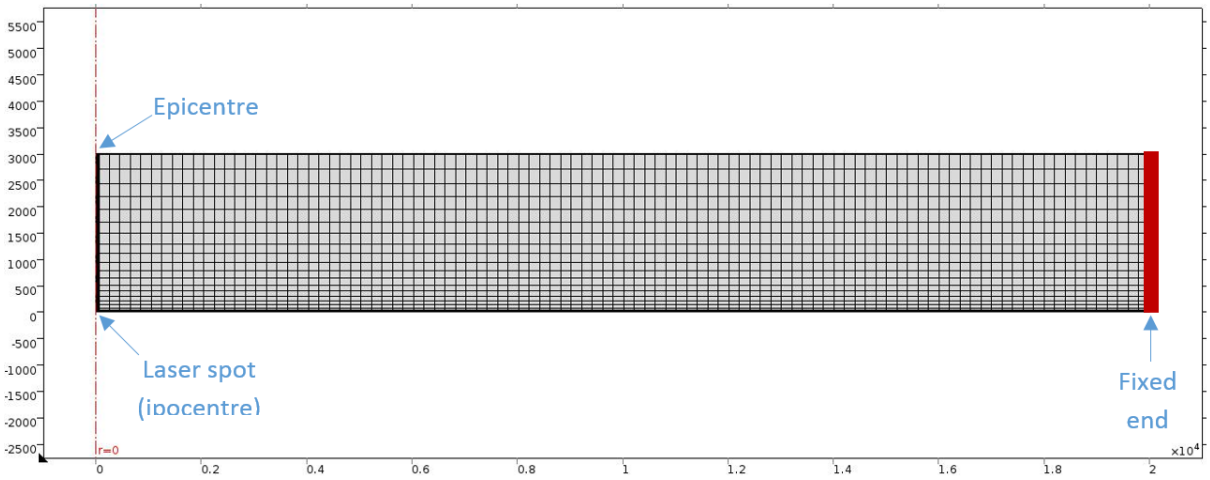

Figure 4. Mesh of the revolution solid with r=20000 µm and z=3000 µm. Along the axis, the laser spot irradiation area (ipocentre) and the epicentre can be seen. A fixed-end constraint is imposed at the edge of the steel disk.

A thermo-elastic coupling for this kind of application is necessary. Above, all letters in bold indicate vectors. The software initially resolves the transient heat-exchange problem through the Fourier equation:

$$\rho c_p \frac{\partial T}{\partial t} + \rho c_p \mathbf{u}\nabla \mathrm{T} = \nabla(\mathrm{k}\nabla \mathrm{T}) + \mathrm{Q}$$

where T is the temperature, t the time, Q is the heat flux (Gaussian profile on the spot), ρ, c_p and k are the material's density, heat capacity at constant pressure and thermal conductivity, respectively. After the determination of temperature distribution in the solid, a generic structural strain ε is calculated as:

$$\varepsilon = \alpha\left(T - T_{ref}\right)$$

where α is the material's linear expansion coefficient and T_{ref} the reference temperature (293 K). The structural mechanics equations used to find the displacement vector $\boldsymbol{u}$ (which represents the elastic waves in the sample) are:

$$\rho \frac{\partial^2 \boldsymbol{u}}{\partial t^2} - \nabla \boldsymbol{\sigma} = \boldsymbol{F_v}, \qquad \boldsymbol{\sigma} = \boldsymbol{S},$$

$$\boldsymbol{S} - \boldsymbol{S_0} = \boldsymbol{C}\colon(\boldsymbol{\varepsilon} - \boldsymbol{\varepsilon_0}),$$

$$\boldsymbol{\varepsilon} = \frac{1}{2}[(\nabla \mathbf{u})^{\mathrm{T}} + \nabla \mathbf{u}],$$

where **C** is the elasticity tensor, '**:**' represents the double dot product, $\boldsymbol{\varepsilon}$ is the strain tensor, $\boldsymbol{\varepsilon_0}$ its initial value (**0**), **σ** the stress tensor and $\boldsymbol{F_v}$ the volume forces vector. In order to obtain a wave propagation which is congruent with the real one, it is necessary [17] to use:

$$t^s_{max} = \frac{1}{180 f_d} \qquad , \qquad l^e_{max} = \frac{\lambda_{min}}{12}$$

where t^s_{max} is the maximum simulation time-step, f_d represents the design frequency (the maximum frequency of interest), l^e_{max} is the maximum length for the finite elements and λ_{min} the minimum ultrasonic wavelength; the latter can be calculated using the minimum speed for the various wave modes v_{min}:

$$\lambda_{min} = \frac{v_{min}}{f_d}.$$

Choosing a f_d value equal to 1 MHz (which is the maximum perceived frequency for the broadband probe), the resulting maximum allowed time-step results in $t^s_{max} = 5.5\ ns$ and then t^s has been set to 5 ns. Since shear waves are the slowest (3100 m/s for steel), $l^e_{max} \cong 234\ \mu m$ and thus the longest element is 200 μm. Only longitudinal waves (L waves) have been studied in this work despite the necessity to represent shear waves.

Ultrasonic probes are sensitive to pressure variations for waves which propagate inside the material; at the exterior, a global displacement is generated with frequency modulations over it. The displacement curves obtained through FE simulations have been filtered considering a low cut-off frequency equal to 100 kHz, so only modulations with frequencies which are inside the probe band are displayed. As can be seen in figure 5 for the epicentre (the disk's opposite point to laser spot), a single laser pulse with a δ equal to 400-800 ns can lead to a first oscillation with high amplitude and a second one which is yet evident. On the other hand, 1200 or 1600 ns long pulses can generate a first oscillation, but there is not a second one. An increase in the oscillation can be highlighted while δ increases, but the maximum oscillation is of the order of $0.1\ pm$. The arrow indicates the ultrasonic time of flight:

$$TOF = \frac{b}{v_l} \cong \frac{0.003\ m}{6000 \frac{m}{s}} = 500\ ns$$

where b is the thickness of the disk (the ultrasonic path) and v_l the longitudinal wave speed (average value for common steel). In the graph, the point where the displacement slope begins demonstrates a good agreement with the calculated TOF value.

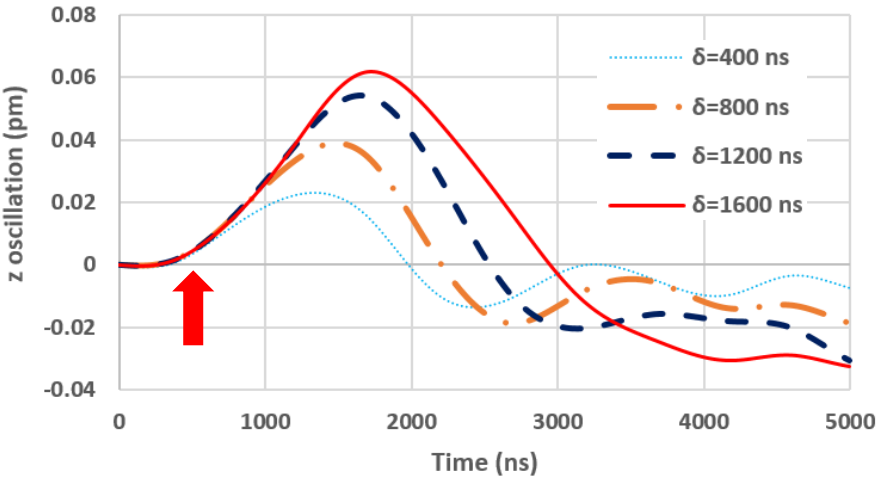

Figure 5. Axial displacement (L wave) at the epicentre as a function of δ (400, 800, 1200, 1600 ns in duration).

A modal analysis has been carried out to find the resonances of the constrained system, resulting in the epicentre maximum displacement for a load frequency of around 300 kHz.

The displacements' frequencies of interest (probe band 0.1-1 MHz) are shown in figure 6. Fast Fourier Transform FFT coefficients are presented as a function of δ, without the zero-frequency term and normalized with respect to the maximum value for the various durations. As can be seen, the normalized coefficients shift towards the low frequencies with increasing δ: the longer the heating period, the lower the value of high frequencies coefficients and vice versa. The change in FFT coefficients for different frequencies as the pulse duration varies means that resonance effects only partially arise due to the thermo-elastic excitation.

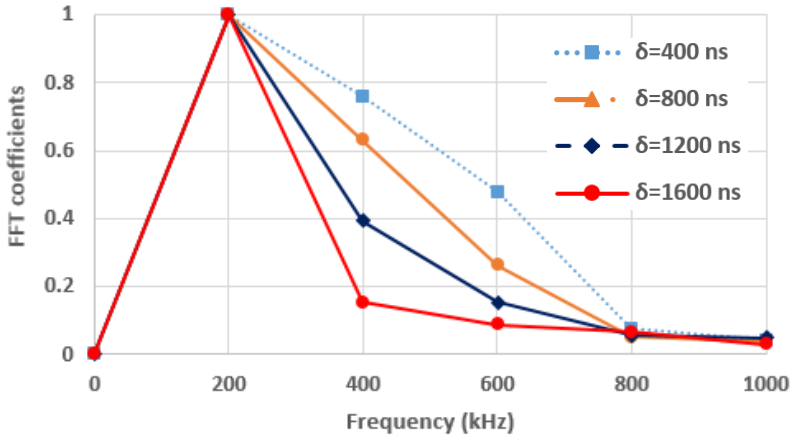

Figure 6. FFT normalized coefficients as a function of frequency and pulse length δ.

In figure 7, the period of the generated US is shown as a function of δ; tracing a $P = \delta$ straight line, it can be shown that the generated ultrasonic wave has a period which is more than double the heating duration δ. In addition to this, P greatly increases as the δ value rises. So, for example, to

create an ultrasonic oscillation period under 2000 ns (US complete sinusoid), a heating period of 1000 ns is not sufficient (laser ON length only).

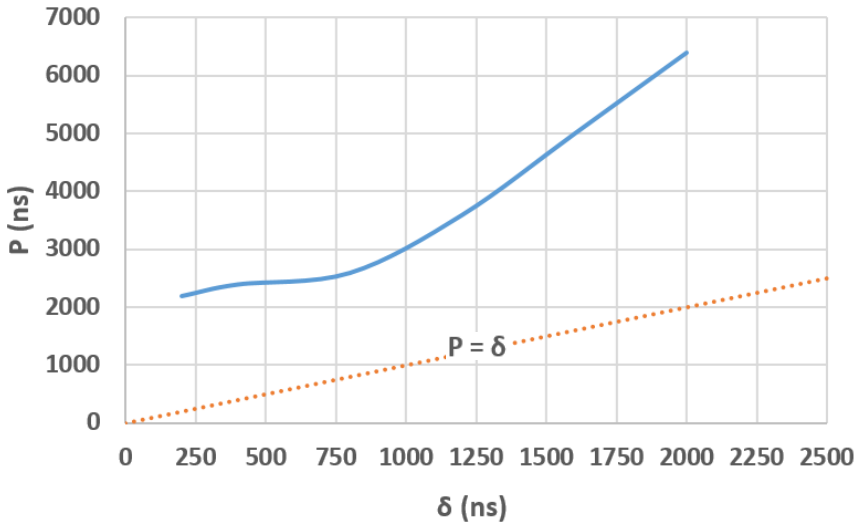

Figure 7. The ultrasonic period P as a function of the pulse length δ.

Multiple pulses are commonly used in experimental testing to increase the amplitude of the generated displacement and to apply post-processing SNR enhancing techniques (i.e. the cross-correlation) [10-12]. As an example, the influence of 3 pulses on the epicentre displacements is shown in figure 8. The pulse durations δ are all the same and equal to 800 ns, but the relative distances are 3200 ns. The TOFs are indicated, as in the single pulse case, with an arrow: the first and third calculated TOFs coincide with the reported ones; the second, though, differs from it: referring to figure 6, an existing oscillation is present in correspondence of this TOF for a single pulse, thus the second generated US interfere with it. If the relative distance between pulses is adequately chosen (i.e. reheating at the minimum of an oscillation), no amplification nor decrease in the displacement is produced, but the US is generated approximately in the same way for every laser pulse.

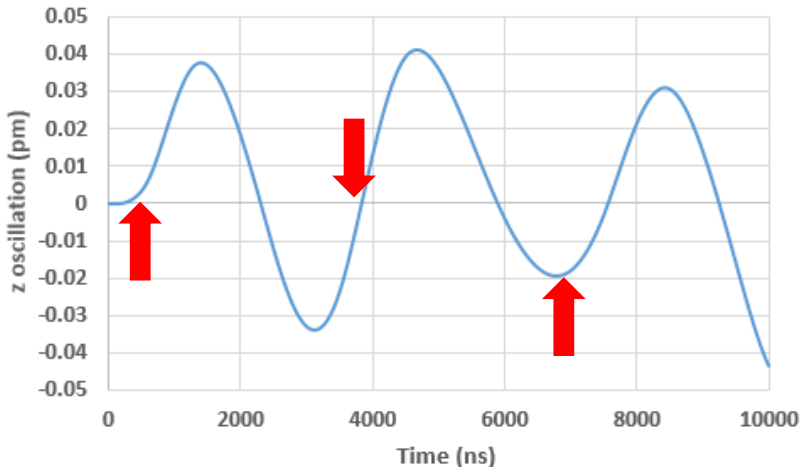

Figure 8. Displacement at the epicentre for a 3 pulses excitation (δ=800 ns).

For the considered 3 pulses excitation, the ultrasonic frequencies generated are reported in figure 9 (not normalized). It can be seen, comparing this curve to the $\delta = 800\ ns$ one in figure 5, a narrowing of the band around 300 kHz, which is also the steel disk resonance frequency.

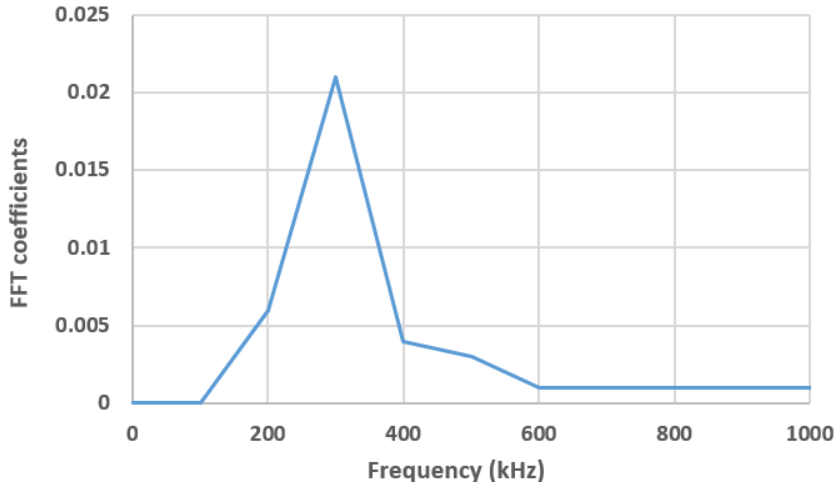

Figure 9. FFT normalized coefficients for a 3 pulses excitation (δ=800 ns) as a function of frequency.

The FE analysis has demonstrated that, effectively, generating a high number of pulses does not increase the oscillations amplitude: preliminarily, it can be assessed that the experimental need to use a high number of pulses is due to post-processing purposes and not for the amplification of oscillations. The use of 3 pulses allows to obtain oscillations around 0.05 pm. If the distance between pulses is adequately imposed, a non-interference condition can be reached between them, thus generating USs with the same characteristics (in particular the main frequency). For the chosen example, though, the main frequency obtained correspond to the resonance one, implying that many conditions regarding different values of δ and distance between pulses should be considered to determine if resonance conditions arise in every case. Simulating them all is not a practical choice. In addition, it was not possible to simulate entire sequences with hundreds or thousands of pulses with HIGHs and LOWs random distribution because of the low time-step, meaning that the influence of interactions between many ultrasounds could not be fully investigated. For all these reasons, the importance of parameters like the pulses lengths, the relative distance between pulses and their number is then determined through experimentation.

4. RESULTS

Experimental tests were carried out to establish how the SNR is influenced by the change in some T sequence parameters. SNR represents how much higher the ultrasonic amplitude is in respect to the noise, thus highlighting how much the US is evident after a post-processing (cross-correlation) procedure.

As displayed in figure 8, the FEM analysis allowed to preliminarily study USs generated through 3, 800 ns long and 3200 ns spaced in time laser pulses. To characterize low-power laser generated US, thus, 3 main parameters must be studied:

1. δ: pulses duration;
2. N_{pulses}: number of pulses contained in the T sequence;
3. d_{pulses}: relative mean distance between pulses.

Several T sequences with different randomness have been generated and studied: the number of LOW levels between pulses ranged between 1 and 5 points for each sequence, but the random spacing was always different for each run. The use of different sequences led though to the same results: hereinafter, thus, only the results for one T sequence will be reported without losing generality.

4.1. Pulse length δ

The pulse length δ determines how much the specimen is heated: the more the heating period, the more the displacement amplitude (but not necessarily the oscillation). As can be seen in figure 10, the SNR increases as δ rises. A T sequence consisting of 2000 pulses has been chosen as a reference. For the highest values of δ, an asymptotic behaviour can be highlighted, probably because the generated US main frequency moves away from the probe band (under 100 kHz). This phenomenon mainly depends on the material characteristics.

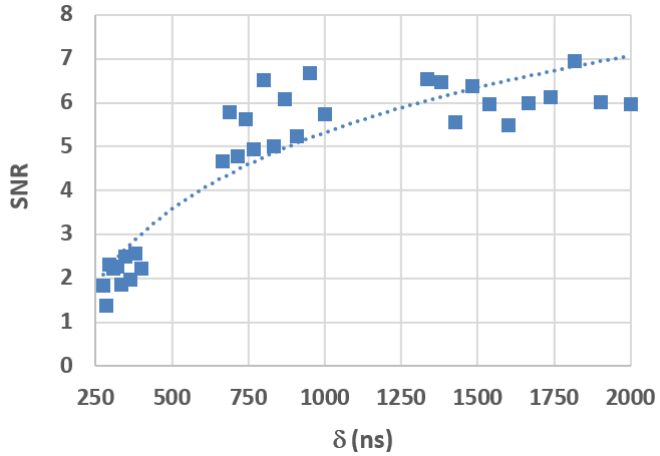

Figure 10. SNR for the T sequence as a function of δ.

Since the change in the ultrasonic frequencies can greatly affect SNR, it is necessary to analyse the frequency composition of the ultrasonic signal resulting from a δ long laser excitation. Figure 11 shows the Fourier coefficients' values corresponding to frequencies between 0 Hz and 1 MHz as a function of δ. Low values of δ imply the US generation with a main frequency band (dark in the figure) with some modulations (more clear and next to it), capable of covering almost the entire probe frequency band; as δ raises, the ultrasonic frequencies reduce, with a band which is very narrow for $\delta = 2000\ ns$: this is perfectly in line with FE simulations for a single pulse.

The ultrasonic main frequencies for $\delta = 2000\ ns$ are extremely close to the lower limit of the band probe, justifying the SNR asymptotic behaviour shown in figure 10. Points in the graphs with amplitude values above 2 can be approximately fitted with a linear trend: it can be an important feature for studies like NDT or material characterization where the suitable ultrasonic frequency choice has a great impact. The frequency composition obtained from the FE model when multiple pulses are used (figure 9) is very similar to the one obtained experimentally. The decrease in the main frequency as δ rises suggests, though, that the correspondence with the resonance frequency is not applicable for all δ values. The resonance, thus, influences only partially the generated US frequency.

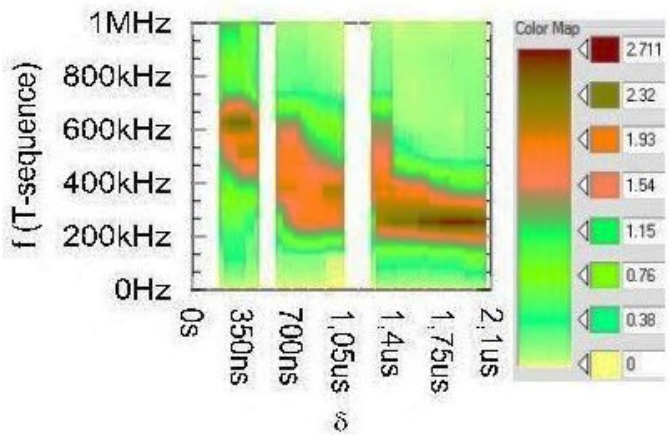

Figure 11. Frequencies and related Fourier coefficients at various δ.

In the end, the use of a high δ is recommended to maximise the SNR, but always keeping in mind that a very high value of this parameter can generate ultrasonic frequencies out of the probe band. If ultrasonic probes with an inferior lower band limit are available (20 kHz), δ can be further increased.

4.2. Number of pulses N_{pulses}

As previously mentioned, the number of pulses is the main parameter which can lead to ultrasonic individuation in real testing campaigns, since a single pulse creates oscillations which are not detectable (tenth of pm). The influence of the pulses number N_{pulses} on the SNR is shown in figure 12, with an imposed δ value equal to 800 ns. The T sequence application allows to obtain a SNR which tends to increase as N_{pulses} raises: this increase is not quick, coherently with FE simulations (figure 8). In fact, the number of pulses is not that important since USs with the same amplitude and frequency are generated at each laser pulse; the increase is mainly due to a major effectiveness of the cross-correlation operation when a large amount of pulses is applied. So, a high number of pulses is desirable to obtain a high SNR. It is however important to underline that the inspected time window widens if many pulses must be used, so also this facet must be considered.

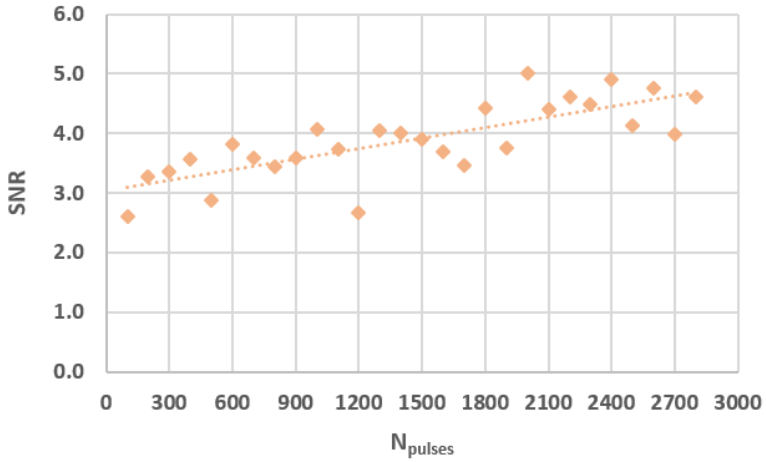

Figure 12. SNR as a function of the number of pulses N_{pulses} with δ equal to 800 ns (inspected time window 8 ms long).

4.3. Distance between pulses d_{pulses}

Another topic which could not be investigated through a FE approach is the influence of the relative distances d_{pulses} for a high number of pulses. Because of the sequences randomness which is necessary to obtain only one and easily characterizable peak in the cross-correlation [15], d_{pulses} represents a mean distance between pulses.

Considering $N_{pulses} = 2000$ and $\delta = 800\ ns$, the trend of SNR is shown in figure 13. An absolute minimum is present around $d_{pulses} = 10\ \mu s$: this is mainly due to the interference between ultrasonic waves generated and reflected at the epicentre (same phase and frequency) caused by the low specimen thickness; a successive minimum (but with a higher SNR) indicates another ultrasonic interference, but between the generated US and the one which has been reflected twice. SNR is high when $\boldsymbol{d_{pulses}}$ is low, meaning that generated and reflected waves do not have the same phase (no ultrasonic interaction). The graph suggests that using pulses relatively close to each other can give better results from a SNR maximization perspective.

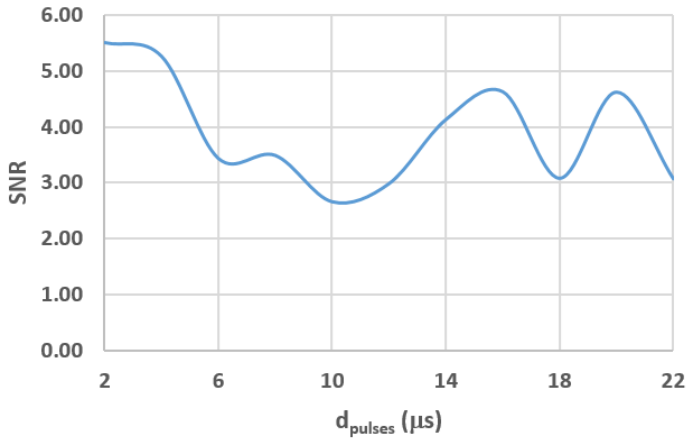

Figure 13. SNR as a function of the mean distance between pulses d_{pulses}, considering $\delta = 800$ ns.

5. CONCLUSIONS

A FEM analysis has been carried out to highlight the main characteristics of low-power laser generated US. Some important parameters' influence was studied preliminarily, as for the pulse length and the application of multiple pulses. Data regarding the generated US show: 1) the low displacements entity, even for high heating period, 2) the decrease in high-frequencies components inside the displacement itself. The FE analysis also showed that a large amount of pulses (with same length) used in testing campaigns increases the number of ultrasonic oscillations generated but not their amplitude, leading to a more easily detectable peak when post-processing techniques (i.e. cross-correlation) are applied.

Starting from the FE results, experimental procedures were applied to highlight the importance of the parameters considered in simulations. Highly random codes are meant to be used as input of the laser modulated diode, to improve the efficiency of the cross-correlation post-processing technique. So, a family of sequences called T sequence (which is not present at the state of the art) has been created.

The results of the application of one particular T sequence are reported for every important parameter considered:

1) δ - The pulse length varies the generated US in two different ways, i.e. changing the US amplitude and frequency content. An increase in δ increases the thermal oscillation and so it allows to obtain a high SNR in general too. However, it is true if the US frequency band is entirely inside the probe band. So, while the carried-out analysis has made use of a broad-band probe which is near the ultrasonic lowest frequency (20 kHz), the use of probes with an inferior lower band limit can lead to an increase in SNR if higher δ are used.
2) N_{pulses}- A very high number of pulses implies a wider inspected time window. Apart from this, high values of this variable are necessary in order to detect the ultrasound and are recommended to obtain good SNRs.
3) d_{pulses}- The T sequence allows to obtain a maximum in SNR when d_{pulses} is very low, while an increase creates a minimum in SNR because of the interference between counter-phase generated and reflected ultrasonic waves; the point where the minimum is found depends on the geometrical and thermo-elastic features of the inspected object.

In conclusion, the FE analysis allowed to adequately comprehend the US thermo-elastic generation phenomenon inside the material. The successive experimentation expanded the study and the phenomenon comprehension evaluating the influence of other parameters through which the CW laser is modulated. The features of the generated US are defined once the parameters defining the input T sequence are chosen and imposed. In the end, the T sequence which allows to obtain the highest SNR is the one with the highest values of N_{pulses} and δ (with ultrasonic frequency inside the probe band) and with the lowest d_{pulses}.

Since input PN codes' influence has not been considered, future studies will take on a comparison between their use and the T sequence one. In addition, only longitudinal waves have been investigated so other works will naturally deal with low-power laser generated surface US and their characteristics.

References

[1] Withers P J et al. 2008 Recent advances in residual stress measurement *International Journal of Pressure Vessels and Piping* **85-3** 118-127
[2] Shaswary E et al. 2015 A new algorithm for time-delay estimation in ultrasonic echo signals *Transactions on Ultrasonics, Ferroelectrics, and Frequency Control* **62-1** 236-241
[3] Scruby C B, Drain L E 1980 *Laser Ultrasonics - Techniques and applications* Ed. Adam Hilger
[4] Singhal M et al. 2006 Characterization of laser generated bulk waves using wavelet transforms and pattern recognition *A-PCNDT*
[5] Cavuto A et al. 2015 Experimental investigation by laser ultrasonics for high speed train diagnostics *Ultrasonics* **55** 48-57
[6] Lee J R et al. 2013 Comparative analysis of laser ultrasonic propagation imaging system with capacitance and piezoelectric air-coupled transducers *Journal of Intelligent Systems and Structures* **3** 551-562
[7] Park, B. et al. 2013 Laser ultrasonic imaging and damage detection for a rotating structure *Structural Health Monitoring* **12-5/6** 494-506
[8] Vangi D et al. 2013 Laser-ultrasound application for train axles monitoring (Applicazione Laser-Ultrasuoni per il Monitoraggio degli Assili Ferroviari) *Proc. of 42nd AIAS Nat. Conf.* 215
[9] Sohn H. et al. 2014 Fatigue crack localization using Laser Nonlinear Wave Modulation Spectroscopy (LNWMS). *Journal of the Korean Society for Nondestructive Testing* **34-6** 419-427
[10] Veres I A et al. 2013 Golay code modulation in low-power laser-ultrasound *Ultrasonics* **53-1** 122-129
[11] Pierce S G, Culshaw B 1998 Laser generation of ultrasonic Lamb waves using low power optical sources *Science, Measurements and Technology* **145-5** 244-249
[12] Anastasi R F, Madaras E I 1999 Pulse Compression Techniques for Laser Generated Ultrasound *Ultrasonics Sym., Proc. of the IEEE* **1** 813-817

[13] Kohanzadeh Y et al. 1974 Thermoelastic waves generated by laser beams of low power *The Journal of Acoustical Society of America* **57-1** 67-71
[14] Cleary A et al 2011 Low power laser generated ultrasound: signal processing for time domain data acquisition *Journal of Physics: CS* **278-1**
[15] Vangi D et al. 2017 Study on the most influential parameters in low-power laser generated ultrasound *FME Transactions* **45** 323-330
[16] Dixon R C 1984 *Spread Spectrum Systems* Ed. J. Wiley
[17] Wang J et al. 2007 Numerical simulation of laser-generated surface acoustic waves in the transparent coating on a substrate by the finite element method *Optics & Laser Technology* **39-1** 21-28
[18] Mineo C et al. 2014 Numerical study for a new methodology of flaws detection in train axles *Ultrasonics* **54-3** 841-849
[19] Liu P et al. 2016 Numerical simulation of damage detection using laser-generated ultrasound *Ultrasonics* **69** 248–258
[20] Vangi D et al. 2016 Noise reduction in ultrasonic signals through cross-correlation algorithms for mechanical components' on-line monitoring (Riduzione del rumore in segnali ultrasonori tramite algoritmi di cross-correlazione per il monitoraggio di componenti in servizio) *Proc. of 45th AIAS Nat. Conf.* 673